AFRL-AFOSR-VA-TR-2016-0119

SINTERING, THERMAL CONDUCTIVITY, OPTICAL AND LASING PROPERTIES

Robert Speyer
GEORGIA INST OF TECH ATLANTA

02/26/2016
Final Report

Air Force Research Laboratory
AF Office Of Scientific Research (AFOSR)/ RTB1
Arlington, Virginia 22203
Air Force Materiel Command

REPORT DOCUMENTATION PAGE

Form Approved
OMB No. 0704-0188

PLEASE DO NOT RETURN YOUR FORM TO THE ABOVE ORGANIZATION.

1. REPORT DATE *(DD-MM-YYYY)*	2. REPORT TYPE	3. DATES COVERED *(From - To)*
01-12-2016	Final	05/01/12 - 10/31/15

4. TITLE AND SUBTITLE
Sintering, Thermal Conductivity, Optical and Lasing Properties of Doped-Lu2O3 Fiberous Transparent Ceramics

5a. CONTRACT NUMBER
FA9550-12-1-0219

5b. GRANT NUMBER

5c. PROGRAM ELEMENT NUMBER

6. AUTHOR(S)
Robert F. Speyer, Professor, School of Materials Science and Engineering

5d. PROJECT NUMBER

5e. TASK NUMBER

5f. WORK UNIT NUMBER

7. PERFORMING ORGANIZATION NAME(S) AND ADDRESS(ES)
Georgia Institute of Technology, School of Materials Science and Engineering
771 Ferst Drive
Atlanta, GA 30332-0245

8. PERFORMING ORGANIZATION REPORT NUMBER

9. SPONSORING/MONITORING AGENCY NAME(S) AND ADDRESS(ES)
Directorate of Aerospace, Chemistry and Materials Science
Air Force Office of Scientific Research
875 North Randolph Street
Suite 325, Room 3026
Arlington, Virginia 22203

10. SPONSOR/MONITOR'S ACRONYM(S)

11. SPONSOR/MONITOR'S REPORT NUMBER(S)

12. DISTRIBUTION/AVAILABILITY STATEMENT
DISTRIBUTION A

13. SUPPLEMENTARY NOTES

14. ABSTRACT
Green processing, sintering and post-HIPing methodologies were developed for producing Lu2O3 ceramics of good transparency, up to 8 mol% Yb2O3, using commercial powders not exposed to further chemical processing. Restricting the extent of sintering to relative densities at the threshold of closed porosity facilitated the highest relative density, highest transparency, post-HIPed specimens. Use of other lot numbers of lutetia, as well as less expensive sources, required a deeper understanding of processing to produce ceramics of equal transparency. Ball milling with stabilized zirconia media yielded nano-scale powder with no measurable impurity aquisition. Spray-drying acetone-based slurries of these powders with soluble organic binder/plasticizer facilitated sintering to a closed porosity state at lower temperatures. Black spots dispersed in otherwise transparent samples required adjustment of O2 thermolysis temperatures to eliminate what was interpreted as carbon char left behind from pyrolysis of processing organic liquids. Suggested follow on work is to change the organic additives and suspending fluid to eliminate these spots, and alteration of pressing conditions, or changing to slip casting, to eliminate large-scale porosity from remnants of spray dried granules.

15. SUBJECT TERMS
ceramic laser, lutetia, sintering, ytterbia doping, transparency, processing

16. SECURITY CLASSIFICATION OF:			17. LIMITATION OF ABSTRACT	18. NUMBER OF PAGES	19a. NAME OF RESPONSIBLE PERSON
a. REPORT	b. ABSTRACT	c. THIS PAGE		22	Robert F. Speyer, Ph.D.
					19b. TELEPHONE NUMBER *(Include area code)* 404-894-6075

Reset

INSTRUCTIONS FOR COMPLETING SF 298

1. REPORT DATE. Full publication date, including day, month, if available. Must cite at least the year and be Year 2000 compliant, e.g. 30-06-1998; xx-06-1998; xx-xx-1998.

2. REPORT TYPE. State the type of report, such as final, technical, interim, memorandum, master's thesis, progress, quarterly, research, special, group study, etc.

3. DATES COVERED. Indicate the time during which the work was performed and the report was written, e.g., Jun 1997 - Jun 1998; 1-10 Jun 1996; May - Nov 1998; Nov 1998.

4. TITLE. Enter title and subtitle with volume number and part number, if applicable. On classified documents, enter the title classification in parentheses.

5a. CONTRACT NUMBER. Enter all contract numbers as they appear in the report, e.g. F33615-86-C-5169.

5b. GRANT NUMBER. Enter all grant numbers as they appear in the report, e.g. AFOSR-82-1234.

5c. PROGRAM ELEMENT NUMBER. Enter all program element numbers as they appear in the report, e.g. 61101A.

5d. PROJECT NUMBER. Enter all project numbers as they appear in the report, e.g. 1F665702D1257; ILIR.

5e. TASK NUMBER. Enter all task numbers as they appear in the report, e.g. 05; RF0330201; T4112.

5f. WORK UNIT NUMBER. Enter all work unit numbers as they appear in the report, e.g. 001; AFAPL30480105.

6. AUTHOR(S). Enter name(s) of person(s) responsible for writing the report, performing the research, or credited with the content of the report. The form of entry is the last name, first name, middle initial, and additional qualifiers separated by commas, e.g. Smith, Richard, J, Jr.

7. PERFORMING ORGANIZATION NAME(S) AND ADDRESS(ES). Self-explanatory.

8. PERFORMING ORGANIZATION REPORT NUMBER. Enter all unique alphanumeric report numbers assigned by the performing organization, e.g. BRL-1234; AFWL-TR-85-4017-Vol-21-PT-2.

9. SPONSORING/MONITORING AGENCY NAME(S) AND ADDRESS(ES). Enter the name and address of the organization(s) financially responsible for and monitoring the work.

10. SPONSOR/MONITOR'S ACRONYM(S). Enter, if available, e.g. BRL, ARDEC, NADC.

11. SPONSOR/MONITOR'S REPORT NUMBER(S). Enter report number as assigned by the sponsoring/ monitoring agency, if available, e.g. BRL-TR-829; -215.

12. DISTRIBUTION/AVAILABILITY STATEMENT. Use agency-mandated availability statements to indicate the public availability or distribution limitations of the report. If additional limitations/ restrictions or special markings are indicated, follow agency authorization procedures, e.g. RD/FRD, PROPIN, ITAR, etc. Include copyright information.

13. SUPPLEMENTARY NOTES. Enter information not included elsewhere such as: prepared in cooperation with; translation of; report supersedes; old edition number, etc.

14. ABSTRACT. A brief (approximately 200 words) factual summary of the most significant information.

15. SUBJECT TERMS. Key words or phrases identifying major concepts in the report.

16. SECURITY CLASSIFICATION. Enter security classification in accordance with security classification regulations, e.g. U, C, S, etc. If this form contains classified information, stamp classification level on the top and bottom of this page.

17. LIMITATION OF ABSTRACT. This block must be completed to assign a distribution limitation to the abstract. Enter UU (Unclassified Unlimited) or SAR (Same as Report). An entry in this block is necessary if the abstract is to be limited.

SINTERING, THERMAL CONDUCTIVITY, OPTICAL AND LASING PROPERTIES OF DOPED-Lu_2O_3 FIBEROUS TRANSPARENT CERAMICS

Final Report

Submitted by:

Robert F. Speyer
Professor
School of Materials Science and Engineering
Georgia Institute of Technology
771 Ferst Drive
Atlanta, GA 30332-0245
Robert.Speyer@mse.gatech.edu

Submitted To:

Dr. Ali Sayir
Program Manager
High Temperature Aerospace Materials
Directorate of Aerospace, Chemistry and Materials Science
Air Force Office of Scientific Research
875 North Randolph Street
Suite 325, Room 3026
Arlington, Virginia 22203

Contents

I Abstract

Green processing, sintering and post-HIP methodologies were developed for producing ceramics of good transparency, up to 8 mol% Yb_2O_3 in Lu_2O_3, using commercial powders not exposed to further chemical processing. Restricting the extent of sintering to relative densities at the threshold of closed porosity facilitated the highest relaltive density, highest transparency, post-HIPed specimens. Use of other lot numbers of lutetia, as well as less expensive sources, required a deeper understanding of processing to produce ceramics of equal transparency. Ball milling with yttria-stabilized zirconia media yielded nano-scale powder with no measurable impurity acquisition. Spray-drying acetone-based slurries of these powders with soluble organic binder/plasticizer facilitated sintering compacts of granulated powder to a closed porosity state at lower temperatures. Black spots dispersed in otherwise transparent samples were a ubiquitous defect; raising the O_2 thermolysis temperature was required to eliminate what were interpreted to be carbon char left behind from pyrolysis of processing organic liquids. Suggested follow on work is to change the organic additives and suspending fluid to eliminate this pyrolysis, and alteration of pressing conditions, or changing to slip casting, to eliminate remnants of spray dried granules in green microstructures, which imbue porosity on two different length scales.

II Background

II.1 Motivation for Lu_2O_3-based Ceramics

Sesquioxide materials such as Y_2O_3, Sc_2O_3, and Lu_2O_3, are promising laser host materials, owing, in part, to their high thermal conductivities (Figure 1); they have attracted

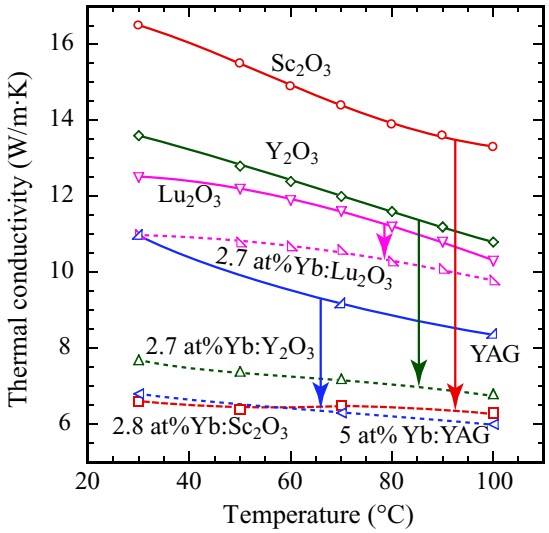

Figure 1: Thermal conductivities with temperature for various sesquioxides in undoped and doped states. Data from Griebner [5].

attention for the development of high output power and ultra short pulsed lasers [1]. Undoped Lu_2O_3, Y_2O_3, and Sc_2O_3 possess higher thermal conductivities and lower CTE's than the well-established yttria-alumina garnet (YAG) laser hosts, which is critical for thermal

management as laser powers are increased and generate more heat during operation [2], especially as laser systems scale toward multi-kilowatt power levels [3]. However, as shown in Figure 1, ytterbium-doping reduced the thermal conductivity of the three sesquioxides, bringing doped Sc_2O_3 and doped Y_2O_3 down to the level of Yb-doped YAG. By contrast, Lu_2O_3 shows only a soft decrease in thermal conductivity with Yb_2O_3 doping. In the case of Sc_2O_3 and Y_2O_3, introduction of the dopant facilitates solid solution phonon scattering with as associated decrease in thermal conductivity. However, ytterbium and lutetium exhibit very similar masses and bonding forces. Thus, Yb^{3+}:Lu_2O_3 is an attractive candidate for high power laser applications because of its inherent heat dissipation capability.

Lutetium oxide adopts a cubic crystal structure and melts at 2490°C. It is insoluble in water but is slightly hygroscopic, and has a high theoretical density (9.420 g/cm^3) [4]. The following literature survey shows the variety of powder synthesis, green processing, and densification heat/pressure treatment methodologies used to form transparent doped Lu_2O_3 laser ceramics. Combinations of these have yielded differing levels of success, as indicated by the approaches to theoretical density and theoretical transmittance (∼80%). These are summarized in Tables 1 through 3.

II.2 Powder Synthesis

Various researchers have found that commercially-available powders of Lu_2O_3 and oxides of the various dopants did not facilitate sintering to the needed transparency [6]. This was overcome via synthesis from solution-precipitated powders. In a synthesis methodology promoted by the Sanghera group at the U. S. Navy Research Laboratory and the Zhou group at Shanghai University, individual oxides were dissolved into hot aqueous nitric acid to form a mixed nitrate solution containing Lu^{3+} plus Yb^{3+} [6, 7, 8, 9], Eu^{3+} [10, 11], Ho^{3+} [12] or Nd^{3+} [13, 14, 15]. Others dissolved chlorides of the starting raw materials (e.g. $LuCl_3$ and $YbCl_3$ [16]). As a compilation of described methods: The solution was filtered (45 μm membrane [10]) to remove insoluble impurities [8]. The precipitate precursor was prepared by adding 250 ml $NH_3{\cdot}H_2O$ (ammonia monohydrate) + NH_4HCO_3 (ammonium bicarbonate) mixed precipitant drop-wise into a 1000 ml mixed solution under mild agitation (magnetic stirrer) [17] (others used ammonium hydroxide [6]). One reference indicated that the precipitation product was $Ln_2(C_2O_4)_3$, where Ln stands for Lu, Yb, Eu, or Nd [11]. In another reference [13], the ultimate pH values of the suspension were kept in the range of 8-9, making sure that all the rare earth cations (Lu^{3+}, Nd^{3+}) had been deposited into precipitate precursors. After being aged for 24 h, the amorphous precursor was filtered using a suction filter, washed four to five times with deionized water and twice with alcohol (others used acetone washings [8]) in attempt to remove any soluble impurities, and then dried at 80°C for 24 h in air. The precipitate was crushed (presumably using an alumina mortar and pestle, but was not specified) and sieved through a 120 mesh (125 μm) screen [13]. Precipitate powders were calcined in various ways: 600°C for 6 h [8], 600-1200°C for 2 h [10], 1000°C with a heating rate of 2°C/min [13]. These were in turn ball milled for 2 h [9, 15] to 48 h [18] in ethanol, yielding nano-scale powder. Zhou et al. suggested that the introduction of CO_3^{2-} was essential to obtain nanosized Lu_2O_3 powders, which arises from the release of CO_2 at ∼700°C during decomposition of the carbonate, preventing the adjacent particles from severe agglomeration [13].

Combustion synthesis methods have been reported in which Lu, Eu, Y, and/or Nd were in the form of chlorides [19] or nitrides [20, 21, 22] in aqueous solution. These were mixed

Table 1: Literature Studies on Fabrication of Transparent Doped Lu_2O_3 (Boulestix 2015 [15], Prakasam 2013 [18], An 2011 [29], Wang 2013 [27], Yanagida 2014 [16], Zych 2012 [21], Zhang 2004 [20], Lu 2002 [19]).

	Dopant	Synthesis	Green Processing	Sintering	Relative Density	Grain Size	Trans-parency	Refer-ence
Spark Plasma Sintered	0.5% Nd	Dissolved in nitric acid. Precipitated with ammonium bicarbonate.	Heated at 900ºC for 2h, particle size 30 nm. Ball milled 2 h in ethanol. Slip cast pellets.	SPS in graphite die, 50 ºC/min to 1400ºC for 15 min, 130 MPa.	?	300 nm	81.4%	Boul-estix 2015
	10% Yb	Dissolved in hot diluted nitric acid (HNO_3), precipitated with NH_4OH to form a precipitate pH = 9. Dried at 100ºC for 2 h.	Ground, then calcined at 600ºC for 12 h. Ball milled in ethanol for 48 h.	Graphite fiber furnace isolation, SPS at 1400-1800ºC. Anneal at 1200ºC, 12 h in air. Best result reached with 1400ºC SPS.	99.5	10 nm - 5 µm	~55%	Pra-ka-sam 2013
	Pure	As-received, 50 nm.	None.	SPS using a graphite liner. 1473ºC 5 min then 1723ºC at various heating rates holding for 45 min.	99.5-100	600-1000 nm	79%	An 2011
	Pure	Purchased (Kojun -do Chemical, Sak- ado, Japan) 50 nm.	None.	SPS 1000-1550ºC, holding from 5-60 min, 10.2 ºC/min.	?	?	?	Guzik 2014
Vacuum Sintered, No HIP	2% Er	As-received.	Ball milled in anhydrous alcohol with 0.5 wt% TEOS sintering aid. ZrO_2 media, 24 h. Calcined 1100ºC, 2 h.	Sintered in vacuum at 1850ºC for 10-12 h.	?	?	67%	Wang 2013
	0.1, 0.3, 1, 3, 100% Yb	Aqueous solution of $LuCl_3$ and $YbCl_3$ (Konoshima Chemical). Precipitation of 100 nm particles by heating suspension. Filtering and washing.	Calcined at ~1000ºC, 24 h ball milling. Cast in a gypsum mold. Organic removed at ? thermolysis temperature.	Vacuum sintered at 1700ºC for 5 h.	?	?	60-80%	Yana-gida 2014
	3,5,7,10 % Eu	Eu and Lu nitrate was mixed with glycerine, NH_2CH_2COOH in water. Mixture was dried and then heated in air to 650ºC to combust to form Lu and Eu oxides.	None	Vacuum sintered at 1700ºC for 5 h.	?	?	?	Zych 2012
	5% Eu	Eu and Lu nitrate was mixed with urea, dried, then combusted in air at 600ºC, and then calcined at 1000ºC.	Ball milled with binder and solvent, pressed into a pellet, and then thermolysis at 600ºC.	Vacuum sintered in a W-mesh furnace < 9.3×10^{-5} Pa at 1700-1800ºC for 4 to 6 h.	?	2-5 µm	?	Zhang 2004
	0.15% Nd	Lu and Nd chlorides mixed with urea in aqueous solution. ~100 nm particles precipitate at 100ºC for 2 h. Filtration and washing with water several times, dried for 2 days at ~120ºC.	Calcined at ~1000ºC to form oxide powder. Ball mill 24 h, then cast into gypsum mold. Thermolysis to remove organics.	Vacuum sintered at ~1700ºC for 5 h.	?	?	?	Lu 2002

Table 2: Literature Studies on Fabrication of Transparent Doped Lu_2O_3, Continued (Seeley 2012 [24], Seeley 2011 [25], Zhou 2009 [13], Zhang 2012 [31], Chen 2006 [17], Shi 2009 [10]).

	Dopant	Synthesis	Green Processing	Sintering	Relative Density	Grain Size	Trans-parency	Refer-ence
Vacuum Sintered, then HIP	$Gd_xLu_{1-x}Eu_{0.1}O_3$ $x = 0$, 0.3,0.6, 0.9,1.0, 1.1	Synthesized by flame pyrolysis at Nanocerox (Ann Arbor, MI). 20 nm.	Aqueous suspension w/ PEG/Darvan, ultrasonicated and shear mixed. Spray dried and sieved (<50 µm). Pressed, thermolysis at 900ºC.	Tungsten furnace, vacuum < 2.7 × 10^{-4} Pa, 1625ºC 2 h to 97% RD. HIPed between 1750 and 1900ºC for 4 h in tungsten element HIP. No post annealing (oxygen bleaching).	?	?	?	See-ley 2012
	5% Eu	Flame spray pyrolysis (Nanocerox).	Aqueous suspension using PEG and Darvan, ultrasonicated + shear mixed, spray dried at 210ºC. Sieved <50 µm, pressed at 50 MPa, thermolysis at 900ºC in air.	Tungsten furnace, <2.7 × 10^{-4} Pa, sintering 1575-1850ºC for 2 h HIPed 200 MPa at 1850ºC for 4 h in tungsten HIP.	99-100	~50 µm	?	See-ley 2011
Flowing H_2 Sintered, No HIP	3% Nd	Lu_2O_3 and Nd_2O_3 dissolved in HNO_3 precipitated via NH_4OH + NH_4HCO_3. Aged for 24 h and filtered via a suction filter, Washed 4-5× with water and 2× with alcohol, dried at 80ºC for 24 h. Crushed and sieved to 120 mesh, calcined at 1000ºC.	Uniaxially pressed into pellets, and CIPed at 200 MPa.	Sintered in a W furnace under flowing H_2 at 1880ºC for 8 h.	99.7	50 µm	~75%	Zhou 2009
	5% Yb	As-received, 10-50 nm mixed w/ZrO_2 media in ethyl alcohol, calcined in air, 1200ºC 10 h.	CIPed at 200 MPa.	Sintered at 1780ºC for 45 h in flowing H_2. No HIPing.	99.4	?	~60%	Zhang 2012
	5% Eu	Lutetium and europium nitrate precipitated via NH_4OH + NH_4HCO_3 under mild agitation at rt. Aged for 24 h and filtered via a suction filter, washed 4-5× with water and 2× with alcohol, dried at 70ºC for 36 h. Crushed w/Al_2O_3 mortar/pestle calcined at 1000ºC for 2 h.	Uniaxially pressed at ~40 MPa and CIPed at 200 MPa.	Sintered under flowing H_2 at 1850ºC for 6 h.	99.9	50-60 µm	~80%	Chen 2006
	5% Eu	Lu and Eu nitrate solution precipitated by ammonium hydroxide and ammonium hydrogen carbonate, precipitation w/magnetic stirrer. Aged 24 h, suction filtered, washed 4× in DI and 2× in ethyl alcohol.	Calcined at 1000ºC to form 30-40 nm particles. Pressed at 30MPa, CIPed at 200 MPa.	Sintered in flowing H_2 (0.5 l/min) at 1850ºC for 2 h with 2 ºC/min heating rate.	99.8	?	80%	Shi 2009

Table 3: Literature Studies on Fabrication of Transparent Doped Lu_2O_3, Continued (Kim 2015 [9], Sanghera 2011 [6], Kim 2013 [12], Zhou 2014 [14], Serivalsatit 2014 [23]).

	Dopant	Synthesis	Green Processing	Sintering	Relative Density	Grain Size	Trans-parency	Refer-ence
Hot Press, then HIP	10% Yb	Dissolved in hot diluted nitric acid (HNO_3), precipitated with NH_4OH. Precipitate washed with DI and acetone.	Calcined powder jet milled (Sturtevant Micronizer), 15-30 g of powder, screened at 16 mesh.	Mixed with sintering aid, graphite foil lined, hot pressed 1500-1700ºC for 2-6 h at 50 MPa. Then HIPed at 1600-1800ºC at 200 MPa for 2 h.	?	?	80%	Kim 2015
	0.1, 1, 2, 5, 8, 10% Yb	Lu and Yb oxides dissolved in hot nitric acid. Solution filtered with 0.45 µm membrane to remove any insoluble impurities and particles. Boiled off to saturation point and cooled. Repeated 3×. Dissolved in DI and precipitated at 60-80ºC with ammonium hydroxide (pH kept between 8.5 and 10). Mixture stirred for h and cooled. Washed with DI 4× and acetone 2×. Dried at 110ºC for 24 h. Then calcined in air at 600ºC for 6 h.	Powder mixed with LiF sintering aid.	Placed in graphite foil lined graphite die and hot pressed at 1500-1700ºC for 2-6 h at 50 MPa. Samples 99% dense. HIPed at 1600-1800ºC in Ar at 200 MPa for 5 h.	~100	5-20 µm	80%	Sanghera 2011
	0.1, 1, 2, 5% Ho	Coprecipitation using ammonium hydroxide precipitant, stirring.	Calcined in air.	Mixed with LiF sintering aid, hot pressed 1300-1700ºC. 99% RD, then HIPed at ?.	99-100	40-50	80%	Kim 2013
	10% Yb	Lu and Eu oxides dissolved in hot nitric acid. Precipitated at 60-80ºC with ammonium hydroxide (pH kept between 8.5 and 10). Washed with DI and acetone. Dried and calcined in air at 600ºC.	Powder mixed with LiF sintering aid.	Placed in graphite foil lined graphite die and hot pressed at 1600ºC for 2 h at 50 MPa. Samples 99% dense. HIPed at 1600ºC in Ar at 200 MPa for 2 h.	~100	20-50 µm	80%	Kim 2011
Two-step Sintering	3% Nd	Oxide powders dissolved in nitric acid, precipitated with $NH_4OH + NH_4HCO_3$.	?	Two step sintering in flowing H_2, 20ºC/min to 1720ºC 15 min, 1620ºC 10 h.	?	400 nm	?	Zhou 2014
	0.25% Er	Lu_2O_3 and erbium nitrate pentahydrate dissolved in nitric acid at 80ºC, precipitated w/ ammonium hydroxide. Precipitates separated by centrifuge, washed with water. Lutetium sulfate formed by dissolving hydroxyl precipitates with sulfuric acid.	Sulfate solution calcined at various temperatures in flowing O_2 to form nanopowder Eu: Lu_2O_3. Pellets pressed without binder, CIPed.	Vacuum 1×10^{-3} Pa, Two step: 1600ºC, immediately dropped to 1500ºC for 20 h. 99% RD, then HIPed at 1800ºC for 8 h (206 MPa).	99-100	16 µm	79%	Serival-satit 2013

with an organic fuel, urea [19, 20, 22] $(NH_2)_2CO$, or glycine [20, 21] NH_2CH_2COOH. The solution was typically dried 100-150°C for 2 h and a solid residue of ∼100 nm particles was deposited. Filtration and washing were repeated several times. The material was then dried for 2 days at ∼120°C. The precursor was then calcined (combustion synthesized) at 650°C by some references [21, 22], ∼750-1500°C in others [19, 20]. These powders were ball milled [20]. One reference indicated that the powder formed by combustion synthesis was strongly agglomerated, which negatively affected the ability to sinter to high transparency [22].

The Ballato group at Clemson [23] formed a Er-doped sulfate solution and then used hexamethyleneteraime (HMT) as the precipitant. They argued that HMT decomposed at elevated temperature into ammonia and formaldehyde, increasing the pH, in turn precipitating the precursor. The sulfate precipitate was calcined at 1100°C to convert to 60 nm Lu_2O_3 particles. The authors argued that the precipitation method led to well-dispersed nanopowders as compared to the hard-aggregated powders based on nitrate solutions.

The Seeley/Payne group at Lawrence Livermore Labs [24] used nanoscale Eu:Lu_2O_3 [25] or Eu:$(Gd,Lu)_2O_3$ [24] nanopowders synthesized by flame spray pyrolysis (Nanocerox, Inc.). This involves combusting aerosols of single-metal and mixed-metal metalloorganic alcohol solutions, with oxygen at 1200-2000°C. Rapid quenching thereafter produces un-agglomerated nanopowders with the same composition as in the original precursor solutions [26].

II.3 Green Processing

Typically, milled nanopowders were placed in steel dies and uniaxially pressed [10, 13, 17, 20, 23, 24, 25], generally followed by a cold isostatic pressing (CIP) step, to form cylindrical disks in the range of 1-2 mm in thickness. In cases in which organic pressing agents were used, a thermolysis step followed. Only one investigator used spray drying to granulate the nanopowder in advance of pressing (suspension with soluble polyethylene glycol as a binder and pressing agent, and ammonium polymethacrylate as a polymeric deflocculating agent, with the suspension mixed and de-agglomerated using an ultrasonic probe and a high shear mixer) [24, 25]. Some investigators formed disk-shaped green bodies via slip casting (gypsum molds) from aqueous suspensions [12, 16, 19]. Slip casting with a well-deflocculated suspension can result in higher green densities than those obtained under high tonnage uniaxial pressing. Generally, sintering aids were avoided for fear of formation of second phases, though in some cases TEOS [27] and LiF [6, 28] were used. These were believed to volatilize out completely during sintering. Transpariences obtained with LiF sintering aid were better than with TEOS, though all other processing parameters were not held equal.

II.4 Thermal Processing

As can be seen in Tables 1 through 3, specimens were sintered through a variety of methods: spark plasma sintering [15, 16, 18, 29], vacuum sintering, without [16, 20, 21, 27, 30] and with [24, 25] post hot isostatic pressing (HIPing), sintering in flowing hydrogen [10, 13, 17, 31], hot pressing [8, 9, 10, 12], and two-step pressureless sintering [14, 23]. Spark plasma sintering (in which a pulsed DC current is generated through a graphite die squeezing a powder compact at elevated temperature) is the only one of the listed methods to yield transparent samples while maintaining grain sizes in the sub-micrometer range. Vacuum sintering without subsequent HIPing generally did not produce transparent samples, with

the exception of the work by Yanagita et al. [16] who precipitated powders from aqueous solutions of chlorides with urea, slip cast parts, and sintered at 1700°C for 5 h. Various Yb^{3+} doping concentrations were used, with 0.3% reaching the theoretical transmission limit (∼80%). No information was disclosed on vacuum level or whether a graphite or a metal (e.g. tungsten) furnace was used.

The Payne/Seeley group out of Lawrence Livermore Labs sintered 5 mol% Eu-doped Lu_2O_3 powder (via flame spray pyrolysis) compacts made from spray dried granules [25]. In this high-quality work, the compacts were vacuum sintered in a tungsten element vacuum furnace at $< 8 \times 10^{-4}$ Pa over a sintering soak temperature range of 1575-1850°C for 2 h, followed by post hot isostatically pressing (HIPing) at 1850°C for 4 h in a tungsten element HIP. As shown in Figure 2, they found that the minimum sintering soak temperature that

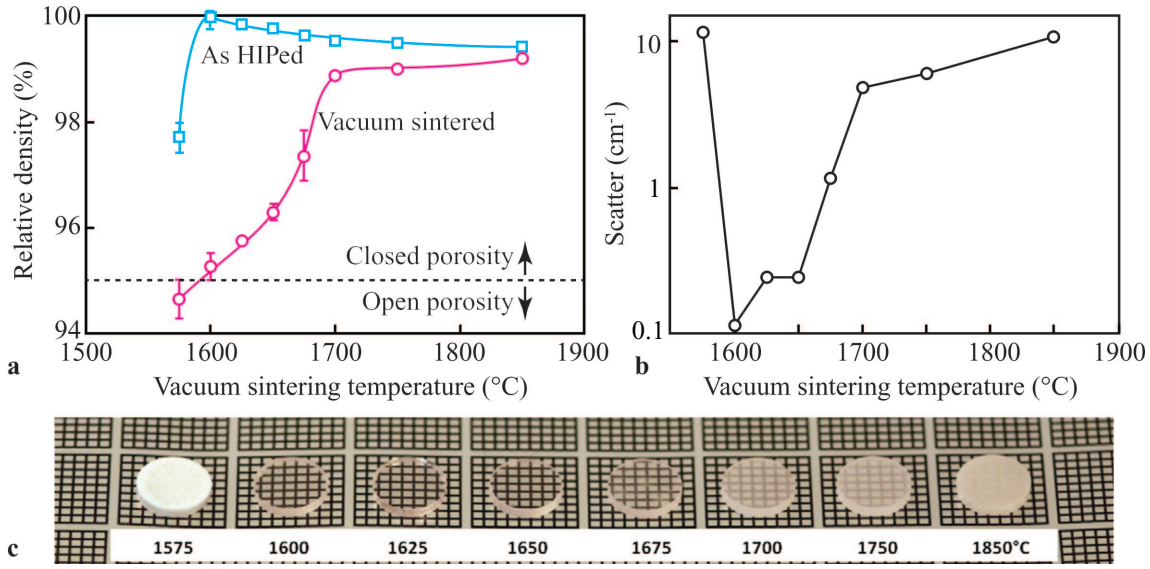

Figure 2: a) Relative densities of 5 mol% Eu-doped Lu_2O_3 [25] after sintering in a tungsten vacuum furnace at various temperatures for 2 h, and then after HIPing in a tungsten hot-zone HIP at 1850°C for 4 h. b) Optical scattering of sintered and post-HIPed specimens exposed to various sintering soak temperatures. c) Appearances of HIPed specimens. After Seeley [25].

yielded closed porosity, resulted in the highest HIPed relative density and transmittance, even though higher sintering soak temperatures yielded higher sintered relative densities. They argued that over-sintering led to rapid grain growth, leaving pores entrapped in grain interiors, which in turn were frozen in place during subsequent HIPing.

The Shi group at the Shanghai Inst. of Ceramics [10, 17] sintered (nitrate solution precipitated) powder compacts in flowing hydrogen at 1850°C, and were able to obtain transmissive polished specimens (text was clearly apparent, but did not appear as cleanly transparent as samples in the Payne/Seeley work). In addition to using H_2 rather than high vacuum, the sintering temperatures were significantly higher and no post-HIPing was used. The authors cite the merits of H_2 sintering based on a classic paper by Coble [32] on the sintering of MgO-doped alumina, in which porosity was eliminated under oxygen and hydrogen atmospheres, but not in N_2, He, or Ar atmospheres, because of the lower diffusivity of these elements through the microstructure.

A method that appeared uniformly successful in obtaining transparent doped Lu_2O_3 was

hot pressing at 1500-1700°C (of chemically co-precipitated powders from nitrate solution), followed by hot isostatic pressing at 1600-1800°C, developed by the Kim/Sanghera group at the Naval Research Laboratory [6, 8, 9, 12]. LiF was used as a sintering aid, which the authors indicated volatilizes away during heat-treatment. It was argued that sintering aids such as lithium fluoride promote etching and removal of impurities in other oxide systems (they detected impurities such as Al, Si, Na, and K). Eu^{3+}, Ho^{3+}, and Yb^{3+} (up to 10 mol% Yb^{3+}) doped Lu_2O_3 were fabricated. They found that jet milling the synthesized powder improved transparency [9].

Following the classic work of Chen and Wang [33], two step sintering was undertaken by the Bellato group [23] at Clemson and the Zhou group [14] at the Shanghai Inst. of Technology. For the Zhou group, sintering at 1720°C for 15 min was followed by cooling to 1620°C, holding for 10 h in a flowing H_2 atmosphere. Final grain size was sub-micron, but no transparency results were provided. In the Ballato work, specimens were heated to 1600°C, and then immediately cooled to 1500°C and held for 20 h under high vacuum (1×10^{-3} Pa). Their intent was to only reach closed porosity, and was subsequently followed by post-HIPing at 1700°C at 206 MPa for 8 h. Their samples were transparent, qualitatively with a slight darkened appearance (transmittance of 78%). The apparent merit of the two step sintering was as it was in the Payne/Seeley group, to sustain minimal grain growth in achieving closed porosity in the sintering step, to facilitate pore removal during the post-HIPing step.

III Results and Discussion

III.1 Initial Work Using Unprocessed Commercial Powders

In our work under AFOSR contract FA9550-12-1-0219, the sinterability of commercial Lu_2O_3 powders with various concentrations of Yb_2O_3 additions was studied. Lu_2O_3 (Alpha Aesar, 99.99% pure, $d_{50} = 4.06$ μm) and Yb_2O_3 (Alpha Aesar, 99.99% pure, < 44 μm) powders (Figure 3) were used to form compositions ranging from 0 to 10 mol% Yb_2O_3. Powders were

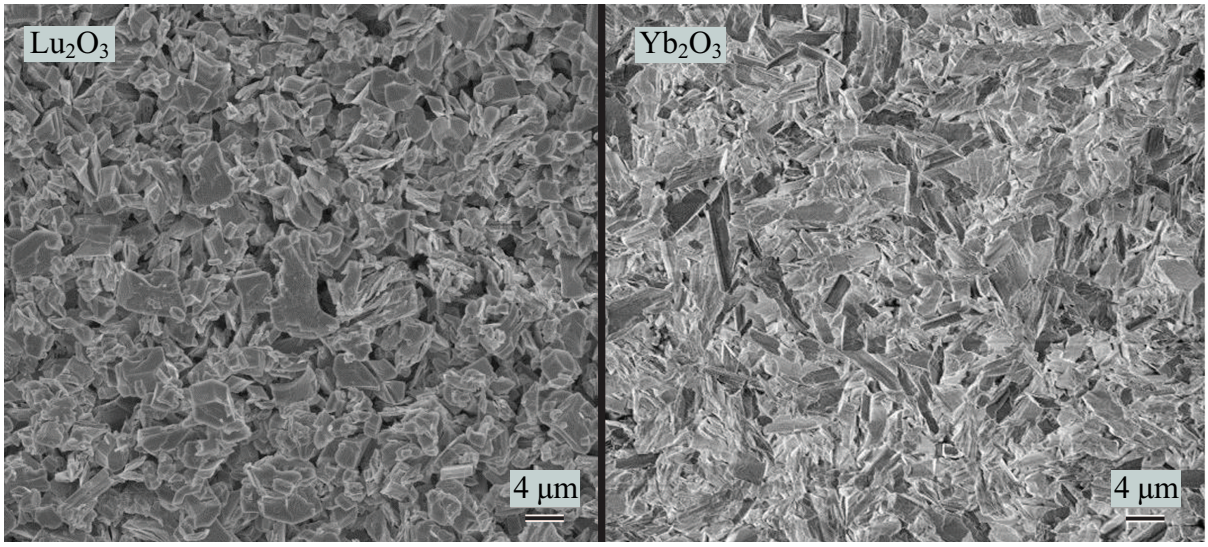

Figure 3: SEM images of Lu_2O_3 (left) and Yb_2O_3 (right) as-received Alfa Aesar powders.

mixed in polyethylene vials on milling rollers, and then uniaxially pressed at 100 MPa into 2

g cylindrical compacts of 12.7 mm in diameter and ∼3.4 mm thickness. The compacts were CIPed at 345 MPa to green relative densities of ∼56%. They were sintered in graphite crucibles in a graphite element vacuum tube furnace (Model M11, Centorr Vacuum Industries, Nashua, NH) under a modest vacuum of ∼3 Pa. Specimens were heated at 50°C/min to selected dwell temperatures in the range 1600-1850°C with durations of 2-4 h. After sintering, many of the specimens had visible colorations, varying from red to yellow, which were successfully removed via annealing in static air at 1100°C for 2 h. They were then HIPed (Model AIP6-30H, American Isostatic Press, Columbus, OH) with argon at 1700°C at 206 MPa for 2 h. In some cases, the pellets were then again similarly annealed in static air at 1100°C for 4 h. Relative densities of the sintered as well as post-HIPed samples were measured using the Archimedes method, along with open and closed porosities, with theoretical densities determined based on the rule of mixtures.

Figure 4 shows the results of sintering and post-HIP heat-treatments on pure Lu_2O_3

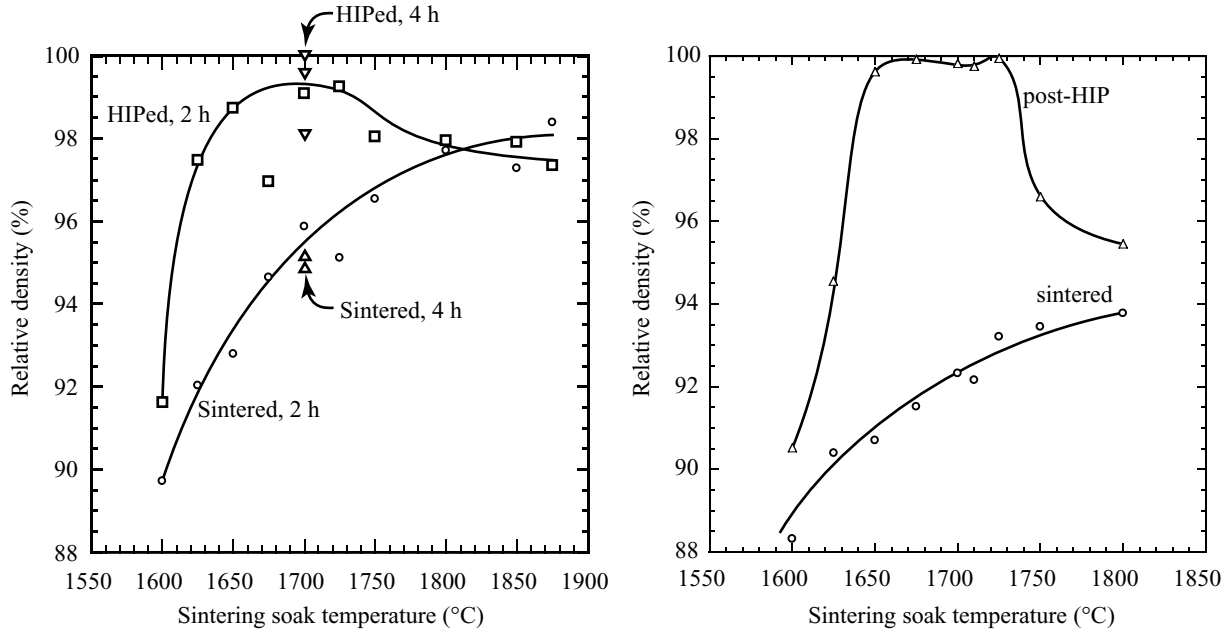

Figure 4: (left) Relative densities of pure Lu_2O_3 specimens after sintering at the indicated soak temperatures and air annealing at 1100°C for 2 h. Also shown are results after these samples were post-HIPed at 1700°C for 2 h and air annealed at 1100°C for 2 h.

Figure 5: (right) Relative densities of 5 mol% Yb_2O_3-doped specimens after sintering and air annealing, and after post-HIPing at 1700°C for 2 h and air annealing, as a function of sintering soak temperature.

samples. Although sintered relative densities generally increased with increasing sintering soak temperature, a peak post-HIPed relative density was reached when specimens were sintered in the soak temperature range of 1650-1725°C. Specimens exposed to sintering soak temperatures above 1800°C gained no apparent relative density benefit from post-HIPing. After post-HIPing compacts exposed to a sintering soak temperature of 1700°C, those soaked for 4 h had higher relative densities than compacts soaked for 2 h.

Figure 5 shows the relative densities of 5 mol% Yb_2O_3-doped specimens exposed to various sintering soak temperatures for 4 h, followed by annealing in static air at 1100°C, post-HIPing at 1700°C for 2 h, and another air annealing at 1100°C. Air annealing had

little measurable effect on relative density. As in the case of pure Lu_2O_3, relative densities increased with increasing sintering soak temperature. Sintering to soak temperatures in the range of 1650-1725°C resulted in ∼100% relative density after post-HIPing. For post-HIPing to be effective, specimens needed to be sintered to a closed porosity state, which was demonstrated to be as low as 90.5% in relative density. Sintering soak temperatures above 1725°C resulted in degraded post-HIPed relative densities, likely from rapid grain growth during sintering which alternately allowed pores to be swept into the grains where they were not effectively eliminated by post-HIPing, or simply aggregated them into larger ones, making their elimination by HIPing more difficult. Typically, post-HIPing is performed 100-200°C below the sintering soak temperature, so that porosity can be eliminated without additional grain growth. For the laser host application; however, grain growth is not a negative so long as it does not affect pore removal. Thus, in this work, there were cases in which the sintering soak temperature was 1650°C, which was followed by post-HIPing at 1700°C; this heat/pressure-treatment resulted in fully dense and transparent post-HIPed specimens. Figure 6 shows the microstructure of a 1725°C sintered and post-HIPed specimen, showing

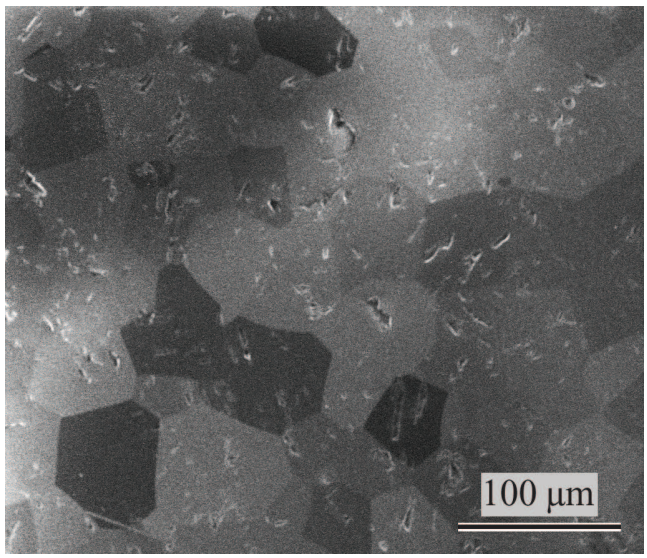

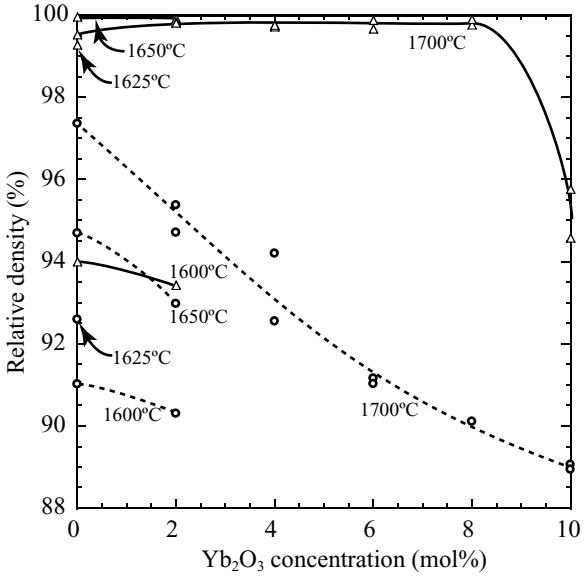

Figure 6: (left) FIB-SEM micrograph of a polished section of a 5 mol% Yb_2O_3 specimen exposed to a sintering soak temperature of 1725°C for 4 h, followed by post-HIPing at 1700°C for 2 h. Differing grain orientations yield contrast after gallium beam etching.

Figure 7: (right) Relative densities of Yb_2O_3-doped specimens after sintering and air annealing, and after post-HIPing (no air annealing after post-HIPing). Sintering soak temperatures are indicated. Circles correspond to sintered relative densities and triangles correspond to post-HIPed relative densities.

grains in the range of 50-80 μm.

Annealing of pellets in ambient air after post HIPing, which were not near 100% relative density, was found to often result in ruptured specimens retrieved from the furnace. Post-HIPing specimens which had remnant open porosity may have trapped compressed argon in what subsequently became closed pores. The ensuing annealing heat-treatment in ambient air permitted the temperature-induced expansion of the entrapped gas to in turn have caused the parts to burst. In some specimens, e.g. the one exposed to a 1700°C sintering soak temperature and no air anneals, opaque grey spheres were observed dispersed within other-

wise transparent specimen interiors. In observing specimens HIPed for 2 h and separately for 4 h, a shrinking core of opaque material could be seen in the process toward forming a uniformly transparent specimen; that is, porosity appeared to be eliminated via HIPing as a progression from the surfaces toward the specimen center. Cross-section microstructures showed a clear interface between dense exterior regions with a pore-containing interior core.

Relative density data for 0-10 mol% Yb_2O_3 doped specimens, using a fixed sintering soak temperature of 1700°C are shown in Figure 7. All but the 10 mol% Yb_2O_3 doped samples post-HIPed to near theoretical density. However, the undoped, 0 and 2 mol% Yb_2O_3 specimens showed relatively degraded transparency. Subsequent heat treatments for 0 and 2 mol% Yb_2O_3 addition compacts with sintering soak temperatures below 1700°C resulted in lower sintered relative densities, but higher post-HIPed relative densities (in the case of a sintering soak temperature of 1650°C). Those specimens in turn displayed good transparency, as can be seen in Figure 8.

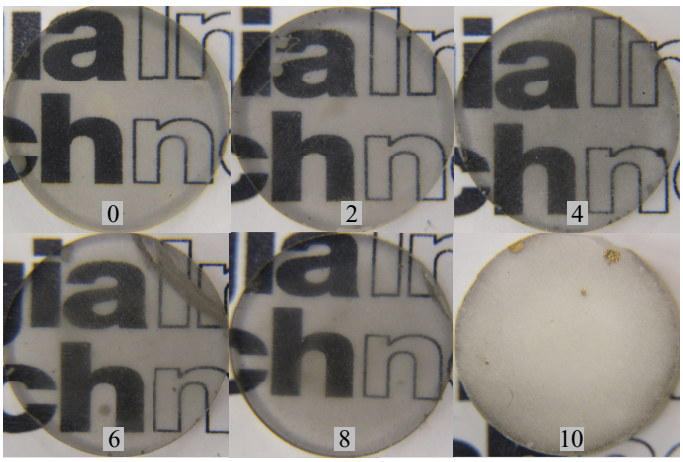

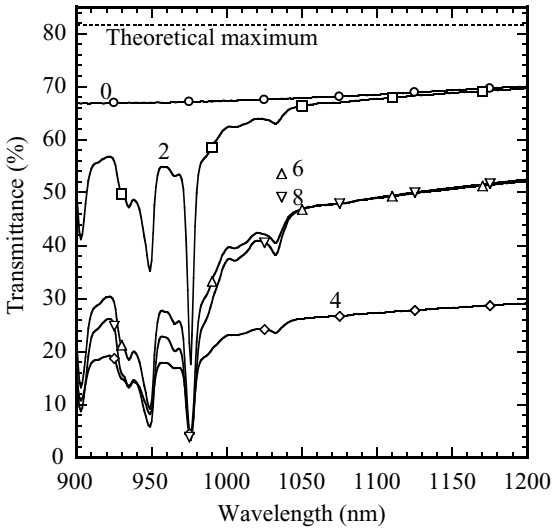

Figure 8: (left) Appearance of polished specimens after exposure to various sintering soak temperatures for 4 h (Yb_2O_3 mol%/sintering soak temperatures in °C: 0/1625, 2/1650, 4/1700, 6/1700, 8/1700, 10/1700), followed by post-HIPing. Numbers in the figure indicate the mol% Yb_2O_3.

Figure 9: (right) : Transmittance spectra. Numbers in the figure indicate Yb_2O_3 concentration in mol%. The theoretical maximum accounts for top and bottom surface reflections.

Transmittance spectra for specimens with Yb_2O_3 contents from 0 to 8 mol% are shown in Figure 9. Spectra were normalized to a thickness of 1.462 mm based on the Beer-Lambert law, and shifted based on calibration from the measured transmittance spectra of a standard absorption filter (Schott neutral glass optical filter, model NG11). Transmittances of 0 and 2 mol% Yb_2O_3 specimens were the best of the series. A grey absorption shifted transmittances down by ∼15% from theoretical limit of ∼82%. Absorption peaks for 2-8 mol% Yb_2O_3 are consistent with those expected from the Yb^{3+} dopant ion.

For this series of specimens, lack of transparency appeared in three forms: a general grey haze, isolated grey spheres, or a yellow appearance. A sintering soak temperature of 1700°C for 0 and 2 mol% Yb_2O_3 yielded the general grey haze, which was visually eliminated by lowering the sintering temperature to 1650°C. The solubility of Yb_2O_3 in Lu_2O_3 appears to be continuous up to 8 mol% Yb_2O_3, as corroborated by x-ray diffraction. At 10 mol%

Yb_2O_3, temperatures may not have been high enough for the two component powders to sinter into such intimate contact so as to facilitate interdiffusion to a single solid solution, though separate diffraction peaks for the two phases were not apparent based on XRD analysis.

III.2 Follow-on Work with Adjusted Processing

With respect to the direct use of commercial powders, the aforementioned work represented an advancement in the levels of transparency which can be achieved. However, as indicated in the literature review, others have attained closer approaches to the theoretical transmittance for doped and undoped Lu_2O_3 by working with chemically precipitated powders. In the present investigation, subsequent lots from the same supplier (Alfa Aesar) required higher ($\sim$125°C) sintering soak temperatures to achieve the highest levels of post-HIPed relative densities and transparency. These optimized heat-treatments yielded specimens with transparencies hampered by more grey haze and localized splotches.

The theme of the follow-on work was to devise a processing strategy that could be economically scaled up based on commercial powders (rather than chemical re-synthesis), and using thermal processing equipment which facilitated net-shape fabrication of larger near-net-shape articles (which may not be as economical; for example, via spark plasma synthesis or hot-pressing). A high purity Lu_2O_3 powder from HEFA Rare Earth (Richmond, BC, Canada), was selected since it was a more price-competitive primary supplier (Alfa Aesar is a re-seller). Initial use of that powder showed similar challenges to uniform transparency as with the later lot numbers of Alfa Aesar powders.

There was a concern that some of the grey haze and splotching observed in the specimens may have been from inadequate vacuum levels, allowing reaction of the furnace structure with available oxygen to form CO gas, which impregnated the densifying sample with carbon. A turbomolecular pump (6.7×10^{-3} Pa) was substituted for the mechanical pump (2.7 Pa) previously used. To eliminate direct contact with potentially reducing graphite, compacts were settered on a larger pre-fired lutetia disk. Post-annealing was performed at 1100°C with a flowing oxygen environment in place of static air.

To reduce particle size, both sonication of an aqueous particle suspension (to break up agglomerates) and particle size separation via aqueous suspension sedimentation were evaluated. Neither had any measurable effect on the sinterability of the powder. Prior attempts at milling the powder with boron carbide or tungsten carbide media resulted in milling media impurity infiltration into the powder (the belief that boron carbide impurity could be oxidized and dissolved out did not bear fruit). However, the use of Y_2O_3-stabilized zirconia media was successful at milling the as-received particles, which were in fact agglomerates of nano-scale particles (Figure 10). X-ray diffraction and SEM EDS analysis of milled powders gave no indication of zirconia impurity. These $\sim$40 nm particles (dried from the milling suspension) did not compact well under uniaxial pressing; green densities were low and sintered parts tended to crack because of non-uniformities in packing density in the compact. As an improvement, the powder was ball milled in an acetone suspension with soluble PMMA (polymethylmethacrylate) binder, and spray dried into spherical granules in a small electrically-heated spray dryer using flowing nitrogen gas and a sonicating nozzle.

These spray-dried granules pressed and sintered well, but HIPing was ineffective. Microstructures of fracture surfaces of sintered specimens showed that the spray-dried granules were not adequately plasticized (outlines of the original granules were apparent in the mi-

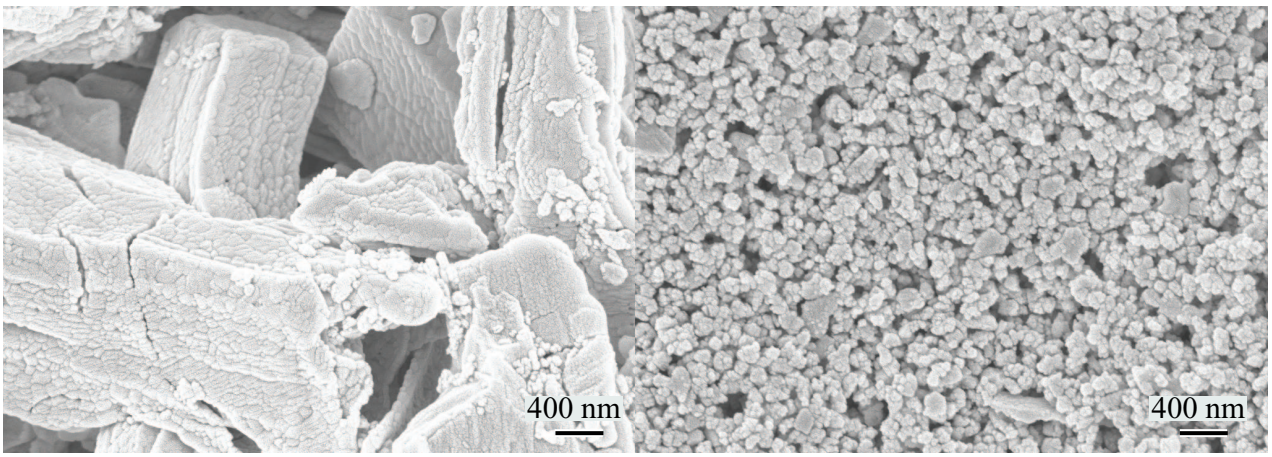

Figure 10: a) As-received HEFA lutetia powder. b) Lutetia powder after ball milling an aqueous suspension for three days in polyethylene jars using stabilized zirconia media.

crostructure). Spray drying was repeated with varying amounts of acetone-soluble dibutyl phthalate used as a plasticizer (which lowers the glass transformation temperature of the PMMA binder). Based on sintered relative density and percent open porosity, an optimized plastizer/binder mass ratio of 0.167 was established. After a thermolysis heat treatment of 1°C/min to 400°C with a 2 h dwell, green relative densities were ∼60%. The plasticizer addition facilitated elimination of open porosity in the sintered part, which in turn facilitated post-HIPing to near-theoretical density. Specimens showed transparency limited by a light grey haze and dispersed black blemishes (Figure 11).

It was believed that a tungsten hot zone and heating element furnace may provide a less chemically-interactive environment for sintering of these specimens to transparency. An older furnace of this type was interfaced with modern controls and values/seals were replaced to bring it to a vacuum-tight condition. In an initial study (Figure 12), sintered relative densities increased relatively monotonically from 92.8% at a sintering soak temperature of 1500°C to 96.0% at a sintering soak temperature of 1750°C. Although Archimedes measurements indicated the closed porosity condition had been reached for all these specimens, HIPing was not successful in fully densifiying them. The best results were for the specimen sintered at 1600°C, when HIPed at 1700°C, which reached a relative density of 99.3%. An impurity phase was visually apparent as a deposit on the surfaces of the specimens. X-ray diffraction confirmed that the phase was Lu_2WO_6 (ICDD: 00-026-0870); the presence of tungsten was further confirmed by SEM EDS.

Specimen compacts were then buried in as-received Lu_2O_3 powder. After sintering heat treatments, this impurity phase deposit appeared on top of the powder, with no deposits visually apparent in the buried samples. Figure 13 shows an extensive matrix of sintering and HIPing temperatures, times, and pressures for buried samples. Only in the case of sintering at 1650°C for 4 or 12 hours, followed by post-HIPing at 1800°C was a close approach to theoretical density achieved. This is in agreement with the results of Payne/Seeley [25]. After O_2 annealing at 1100°C for 2 h, splotches were not apparent, though transparency was interrupted by a light haze (Figure 14).

The change to the tungsten heating element furnace was initially motivated by the belief

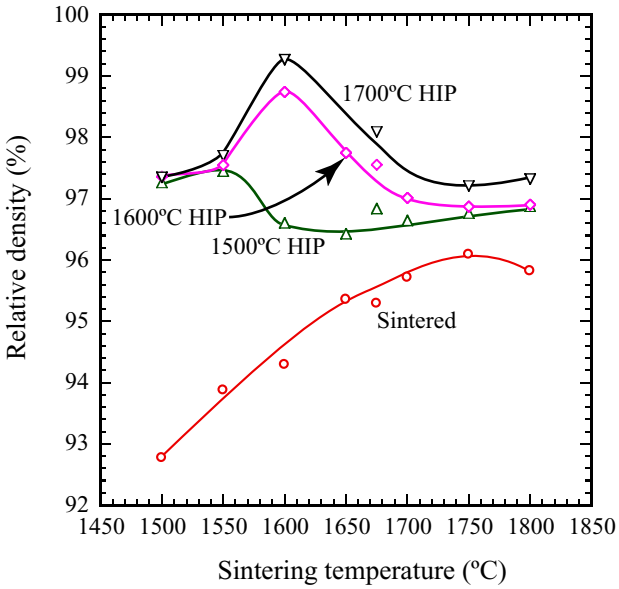

Figure 11: (left) Specimen sintered at 1600°C in the graphite heating-element furnace for 4 h and post-HIPed at 1600°C for 4 h, to a relative density of 99.60%.

Figure 12: (right) Relative densities of specimens sintered in a tungsten heating-element furnace at temperatures as indicated on the x-axis, and post-HIPed at various temperatures.

that the visually-apparent black spots dispersed throughout the microstructure were caused via deposition of graphite from the graphite furnace structure. These spots were in fact still observed in specimens sintered in the tungsten heating element furnace. Focus shifted to the possibility that a graphite bearing species was introduced during green processing. Thermolysis heat-treatment in flowing oxygen had been performed at 400°C for 2 h. As shown in Figure 15, thermolysis heat treatments at 800°C for 6 h, and at 900°C for 6 h (all followed by sintering and post-HIP processing) eliminated the presence of the black spots. It is speculated that the acetone used as the solvent/suspending agent for spray drying was the source of carbon. Acetone, when combusted in an oxygen-deficient environment can leave a carbon char behind as a pyrolysis product. The spray drying chamber, which starts as air, but becomes oxygen deficient as nitrogen is blown through it during spray drying, may have created such conditions. As a separate development, by immersing specimens in lutetia powder (inside tungsten crucibles) while in the HIP permitted post-HIP temperatures of 1850°C to be used without the significant darkening effects previously encountered at these HIP temperatures (Figure 15c).

What remained was an inconsistently-located white haze in post-HIPed specimens, as depicted in Figure 16. Generally, near-edge regions showed transparency while center regions were opaque, but that was not always the case. It is interpreted that this was a result of non-uniform particle packing density in the as-pressed state. Under uniaxial pressing, regions near the die wall can experience higher pressures since the die wall impedes lateral motion of particles relative to the pressing direction of the punch. The tighter packing of those regions in the green state likely facilitated greater consolidation of spray dried granules, in turn permitting those regions to sinter to a higher relative density, more transparent state. In the cases in which transparency appeared at an asymmetrical location in the disk (Figure 16d),

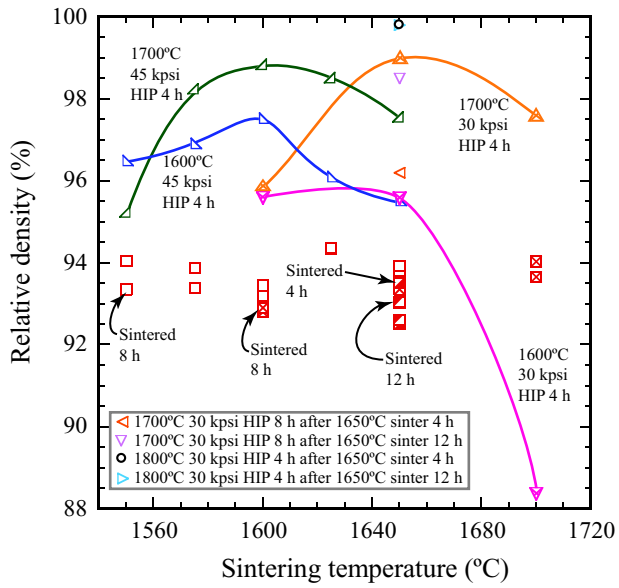

Figure 13: (left) Combinations of sintering and post-HIPing temperatures and soak periods. Open, and cross-hatched symbols for sintering correspond to open and cross-hatched symbols for post-HIPing, respectively.

Figure 14: (right) Appearance of Lu_2O_3 specimen after sintering at 1650°C, buried in Lu_2O_3 powder in the tungsten furnace, followed by post-HIPing at 1850°C for 4 h. Left is after removal from the HIP and polishing. Right is after post annealing in flowing O_2 at 1100°C.

non-uniform die fill may have left a mound in that region, which in turn pressed to a higher green density state at the expense of the remaining volume of the compact. While partially mitigating non-uniform compaction, the CIPing step is interpreted to not have completely eliminated the non-uniform compaction of the uniaxial pressing step.

Studying microstrucural evolution during the sintering heat-treatment (Figure 17) reveals densification on two different lengths scales. The ∼100 nm particles show significant consolidation after the 900°C thermolysis heat-treatment in flowing oxygen, and further densification after heating to 1200°C in vacuum. Above that temperature, abnormal grain growth accelerates. At lower magnification, regions which appear as incompletely merged spray dried particles are apparent, even in the microstructure of the green body. These resisted consolidation until temperatures in the range of 1700°C, at which point they became bands of higher pore concentration among substantially coarsened grains.

IV Recommended Follow-on Work

Elimination of Carbon: The black spots distributed in optical views of specimens was eliminated via a higher temperature (900°C) O_2 thermolysis heat treatment. The removal of these agglomerated carbon-rich regions likely left porosity behind on a size scale of an order of magnitude or more greater than the interparticle porosity. The carbon was either from the binder/plasticizer system (polymethylmethacrylate/dibutyl phthalate), or more likely from partial combustion (pyrolysis) of the acetone solvent/suspending fluid in the oxygen-deficient spray drying atmosphere. Experiments to replace the binder/plasticizer system with polyethylene glycol (PEG-400) and the acetone solvent

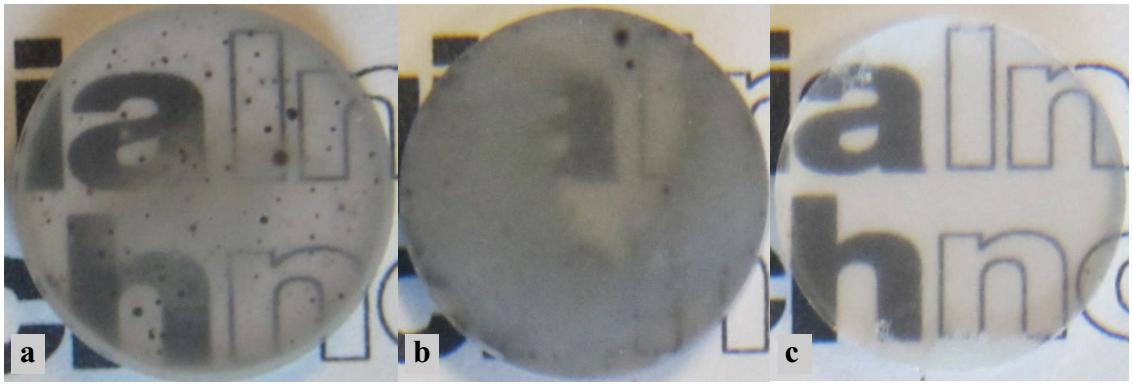

Figure 15: Specimens exposed to varying flowing O_2 thermolysis schedules, showing decreasing concentration of dark spots with increasing thermolysis soak temperatures. a) 400°C for 2h in flowing O_2, followed by vacuum sintering at 1600°C for 8 h, and post-HIPing at 1600°C for 4 h. b) 800°C for 6 h in flowing O_2, followed by vacuum sintering at 1800°C for 15 min, and post-HIPing at 1700°C for 4 h. c) 900°C for 6 h in flowing O_2 followed by vacuum sintering at 1600°C for 4 h and post-HIPing at 1850°C for 4 h.

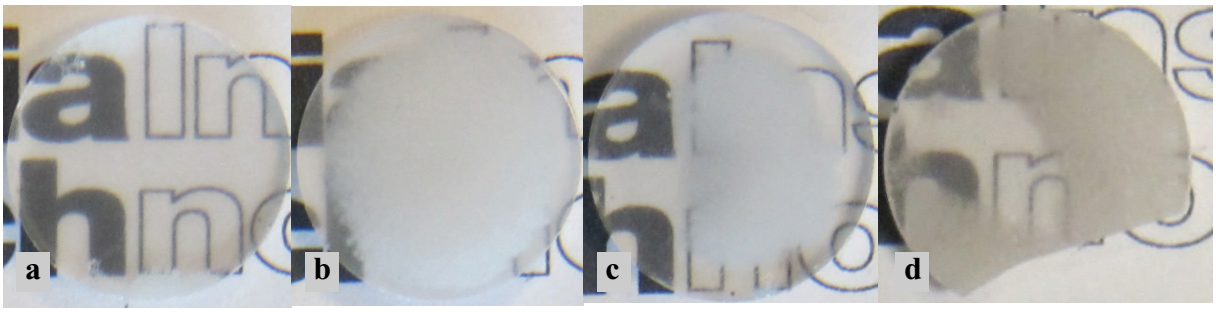

Figure 16: Inconsistent transparency, interpreted to result from non-uniform packing density after uniaxial pressing. Relative densities: a) 99.91%. b) 98.90%. c) 99.53%. d) 99.48%.

with non-pyrolyzing deionized water or ethanol is recommended.

Development of Uniform Green-Body Microstructures: The large-scale intermittent porosity developed from incomplete consolidation of spray dried granules during pressing must be eliminated. Variables for study are uniaxial pressing pressures, binder/plasticizer ratio and content, pressing temperature, vibration to improve and unify powder tap density in the die, and direct isopressing. As an alternative, slip casting well-deflocculated suspensions should form casts with interparticle spacings all on the same length scale. Deflocculation strategies involve pH shifts away from the isoelectric point, and incorporation of soluble polymeric additives which facilitate electrosteric repulsion.

References

[1] A. Ikesue and Y. Aung, "Ceramic Laser Materials," *Nature-Photonics*, **2** 721-727 (2008).

[2] K. Serivalsatit, B. Kokuoz, B. Yazgan-Kokuoz, M. Kennedy, and J. Ballato, "Synthesis, Processing, and Properties of Submicrometer-Grained Highly Transparent Yttria Ceramics," *J. Am. Ceram. Soc.,* **93** [5] 1320-25 (2010).

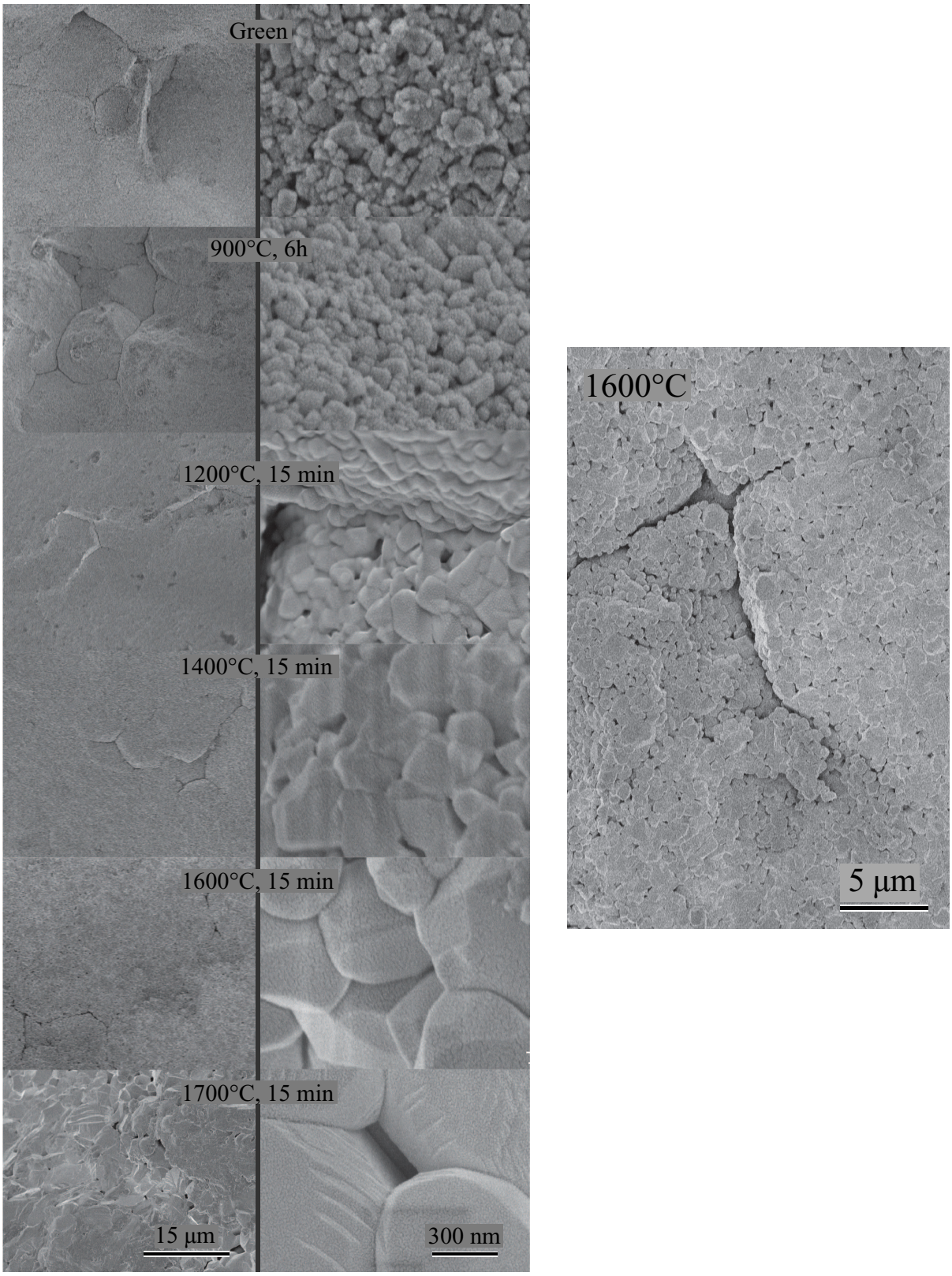

Figure 17: Left: Microstructures viewed at two different magnifications as a function of vacuum sintering dwell temperatures. Heat treatment at 900°C for 6 h was the thermolysis treatment under flowing O_2. Right: Partially-sintered microstructure showing large fissures corresponding to remnants of spray-dried granules.

[3] K. Serivalsatit and J. Ballato, "Submicrometer Grain-Sized Transparent Erbium-Doped Scandia Ceramics," *J. Am. Ceram. Soc.,* **93** [11] 3657-3662 (2010).

[4] http://www.wolframalpha.com/entities/chemicals/lutetium(iii)_oxide/5h/go/jv/.

[5] U. Griebner, V. Petrov, K. Petermann, and V. Peters, "Passively Mode-Locked Yb:Lu_2O_3 Laser," *Optics Express,* **12** [14] 3125-3130 (2004).

[6] J. Sanghera, W. Kim, C. Baker, G. Villalobos, J. Frantz, B. Shaw, A. Lutz, B. Sadowski, R. Miklos, M. Hunt, F. Kung, I. Aggarwal, "Laser Oscillation in Hot Pressed 10% Yb^{3+}:Lu_2O_3 Ceramic," *Optical Materials*, **33** 670-674 (2011).

[7] J. Sanghera, W. Kim, G. Villalobos, C. Baker, J. Frantz, B. Shaw, S. Bayya, B. Sadowski, M. Hunt, and I. Aggarwal, "Transparent Ceramics for High-Power Solid State Lasers," *Laser Technology for Defense and Security VII*, edited by M. Dubinskii, and S. G. Post, *Proc. of SPIE* **8039**, 1-8 (2011).

[8] W. Kim, C. Baker, G. Villalobos, J. Frantz, B. Shaw, A. Lutz, B. Sadowski, F. Kung, M. Hunt, J. Sanghera, and I. Aggarwal, "Synthesis of High Purity Yb^{3+}-Doped Lu_2O_3 Powder for High Power Solid-State Lasers," *J. Am. Ceram. Soc.*, **94** [9] 3001-3005 (2011).

[9] W. Kim, C. Baker, G. Villalobos, J. Frantz, B. Shaw, B. Sadowski, M. Hunt, I. Aggarwal, and J. Sanghera, "Highly Transparent Ceramics Obtained from Jet Milled Sesquioxide Powders Synthesized by Coprecipitation Method," *Optical Materials Express*, **4** [12] 2497-2503 (2014).

[10] Y. Shi, Q. W. Chen, J. L. Shi, "Processing and Scintillation Properties of Eu^{3+} Doped Lu_2O_3 Transparent Ceramics," *Optical Materials,* **31** 729-733 (2009).

[11] A. Lempicki, C. Brecher, P. Szupryczynski, H. Lingertat, V. V. Nagarkar, S. V. Tipnis, S. R. Miller, "A New Lutetia-Based Ceramic Scintillator for X-ray Imaging," *Nuclear Instruments and Methods in Physics Research A,* **488** 579-590 (2002).

[12] W. Kim, C. Baker, S. Bowman, C. Florea, G. Villalobos, B. Shaw, B. Sadowski, M. Hunt, I. Aggarwal, and J. Sanghera, Laser Oscillation from Ho^{3+} Doped Lu_2O_3 Ceramics," *Optical Materials Express*, **3** [7] 913-919 (2013).

[13] D. Zhou, Y. Shi, J. Xie, Y. Ren, and P. Yun, "Fabricaton and Luminecent Properties of Nd^{3+}-Doped Lu_2O_3 Transparent Ceramics by Pressureless Sintering," *J. Am. Ceram. Soc.*, **92** [10] 2182-2187 (2009).

[14] D. Zhou, Y. Ren, J. Xu, Y. Shi, G. Jiang, and Z. Zhao, Fine-grained Nd^{3+}:Lu_2O_3 Transparent Ceramic with Enhanced Photoluminescence," *J. Europ. Ceram. Soc.*, **34** [8] 2035-2039 (2014).

[15] R. Boulestix, R. Epherre, S. Noyau, M. Vandenhende, A. Maitre, C. Salle, G. Alombert-Goget, Y. Guyot, and A. Brenier, "Highly Transparent Nd:Lu_2O_3 Ceramics Obtained by Coupling Slip-Casting and Spark Plasma Sintering," *Scripta Materiala*, **75** 54-57 (2014).

[16] T. Yanagida, Y. Fujimoto, H. Yagi, T. Yanagitani, "Optical and Scintillation Properties of Transparent Ceramic Yb:Lu_2O_3 with Different Yb Concentrations," *Optical Materials*, **36** [6] 1044-1048 (2014).

[17] Q. Chen, Y. Shi, L. An, J. Chen, and J. Shi,"Fabrication and Photoluminescence Characteristics of Eu^{3+}-Doped Lu_2O_3 Transparent Ceramics," *J. Am. Ceram. Soc.*, **89** [6] 2038-2042 (2006).

[18] M. Prakasam, O. Viraphong, D. Michau, P. Veber, M. Velazquez, K. Shimamura, A. Largeteau, "Yb^{3+} Doped Lu_2O_3 Transparent Ceramics by Spark Plasma Sintering," *Ceramics International*, **39** [2] 1307-1313 (2013).

[19] J. Lu, K. Takaichi, T. Uematsu, A. Shirakawa, M. Musha, and K. Ueda, H. Hagi, T. Yanagitani, and A. A. Kaminskii, "Promising Ceramic Laser Material: Highly Transparent Nd^{3+}:Lu_2O_3 Ceramic," *Applied Physics Letters*, **81** [23] 4324-4326 (2002).

[20] K. Zhang, A. K. Pradhan, G. B. Loutts, U. Roy, Y. Cui, and A. Burger, "Lu_2O_3:Eu^{3+} Nanoparticles and Processed Ceramics: Sturctural and Spectroscopic Studies," *J. Mater. Res.*, **19** [9] 2714-2718 (2004).

[21] E. Zych, D. Hreniak, W. Strek, "Spectroscopy of Eu-doped Lu_2O_3-Based X-ray Phosphor," *J. Alloys and Compounds*, **341** [1-2] 385-390 (2002).

[22] E. Zych, D. Hreniak, W. Strek, L. Kepinski, K. Domagala, "Sintering Properties of Urea-Derived Lu2O_3-based Phosphors," *J. Alloys and Compounds*, **341** [1-2] 391-394 (2002).

[23] K. Serivalsatit, T. Wasanapiarnpong, C. Kucera, J. Ballato, "Synthesis of Er-Doped Lu_2O_3 Nanoparticles and Transparent Ceramics," *Optical Materials*, **35** [7] 1426-1430 (2013).

[24] Z. M. Seeley, Z. R. Dai, J. D. Kuntz, N. J. Cherepy, S. A. Payne, "Phase Stabilization in Transparent Lu_2O_3:Eu Ceramics by Lattice Expansion," *Optical Materials,* **35** [1] 74-78 (2012).

[25] Z. M. Seeley, J. D. Kuntz, N. J. Cherepy, and S. A. Payne, "Transparent Lu_2O_3:Eu Ceramics by Sinter and HIP Optimization, *Optical Materials*, **33** 1721-1726 (2011).

[26] http://www.nanocerox.com/flame_spray_pyrolysis.htm.

[27] N.-L. Wang, X.-Y. Zhang, P.-E. Wang, "Fabrication and Spectroscopic Characterization of Er^{3+}:Lu_2O_3 Transparent Ceramics, *Materials Letters*, **94** 5-7 (2013).

[28] A. Krell, T. Hutzler, J. Klimke, "Defect Strategies for an Improved Optical Quality of Transparent Ceramics," *Optical Materials,* **38** 61-74 (2014).

[29] L. An, A. Ito, and T. Goto, "Two-Step Pressure Sintering of Transparent Lutetium Oxide by Spark Plasma Sintering," *J. Europ. Ceram. Soc.*, **31** [9] 1597-1602 (2011).

[30] J. Lu, K. Takaichi, T. Uematsu, A. Shirakawa, M. Musha, and K. Ueda, "Promising Ceramic Laser Material: Highly Transparent Nd^{3+}:Lu_2O_3 Ceramic," *Appl. Phys. Lett.*, **81** [23] 4324-4326 (2002).

[31] H. Zhang, Q. Yang, S. Lu, and Z. Shi, "Structural and Spectroscopic Characterization of Yb^{3+} Doped Lu_2O_3 Transparent Ceramics, *Optical Materials*, **34** [6] 969-972 (2012).

[32] R. L. Coble, "Sintering Alumina: Effect of Atmospheres," *J. Am. Ceram. Soc.*, **45** [3] 123-127 (1962).

[33] I.-W. Chen and X.-H. Wang, "Sintering Dense Nanocrystalline Ceramics Without Final State Grain Growth," *Nature,* **404** [9] 168-171 (2000).

[34] A. Ikesue, Y. L. Aung, T. Taira, T. Kamimura, K. Yoshida, and G. L. Messing, "Progress in Ceramic Lasers," *Annu. Rev. Mater. Res.,* **36** 397-429 (2006).

[35] A. Ikesue, T. Kinoshita, K. Kamata, and K. Yoshida, "Fabrication and Optical Properties of High-Performance Polycrystalline Nd:YAG Ceramics for Solid-State Lasers," *J. Am. Ceram. Soc.,* **78** [4] 1033-40 (1995).

[36] A. Ikesue and Y. L. Aung, "Synthesis and Performance of Advanced Ceramic Lasers," *J. Am. Ceram. Soc.*, **89** [6] 1936-1944 (2006).

[37] Prof. Romain Gaume, University of Central Florida, private communication, January 2016.

[38] L. Jin, G. Zhou, S. Shimai, J. Zhang, S. Wang, "ZrO_2-Doped Y_2O_3 Transparent Ceramics via Slip Casting and Vacuum Sintering," *J. Europ. Ceram. Soc.*, **30** 2139-43 (2010).

1.

1. Report Type

Final Report

Primary Contact E-mail
Contact email if there is a problem with the report.

robert.speyer@mse.gatech.edu

Primary Contact Phone Number
Contact phone number if there is a problem with the report

404-894-6075

Organization / Institution name

Georgia Inst. of Technology

Grant/Contract Title
The full title of the funded effort.

Sintering, Thermal Conductivity, Optical and Lasing Properties of Doped-Lu2O3 Fiberous Transparent Ceramics

Grant/Contract Number
AFOSR assigned control number. It must begin with "FA9550" or "F49620" or "FA2386".

FA9550-12-1-0219

Principal Investigator Name
The full name of the principal investigator on the grant or contract.

Robert F. Speyer

Program Manager
The AFOSR Program Manager currently assigned to the award

Ali Sayir

Reporting Period Start Date

05/01/12

Reporting Period End Date

10/31/15

Abstract

Green processing, sintering and post-HIPing methodologies were developed for producing Lu2O3 ceramics of good transparency, up to 8 mol% Yb2O3, using commercial powders not exposed to further chemical processing. Restricting the extent of sintering to relative densities at the threshold of closed porosity facilitated the highest relative density, highest transparency, post-HIPed specimens. Use of other lot numbers of lutetia, as well as less expensive sources, required a deeper understanding of processing to produce ceramics of equal transparency. Ball milling with stabilized zirconia media yielded nano-scale powder with no measurable impurity aquisition. Spray-drying acetone-based slurries of these powders with soluble organic binder/plasticizer facilitated sintering to a closed porosity state at lower temperatures. Black spots dispersed in otherwise transparent samples required adjustment of O2 thermolysis temperatures to eliminate what was interpreted as carbon char left behind from pyrolysis of processing organic liquids. Suggested follow on work is to change the organic additives and suspending fluid to eliminate these spots, and alteration of pressing conditions, or changing to slip casting, to eliminate large-scale porosity from remnants of spray dried granules.

Distribution Statement
This is block 12 on the SF298 form.

Distribution A - Approved for Public Release

Explanation for Distribution Statement

If this is not approved for public release, please provide a short explanation. E.g., contains proprietary information.

SF298 Form

Please attach your SF298 form. A blank SF298 can be found here. Please do not password protect or secure the PDF The maximum file size for an SF298 is 50MB.

Speyer-SF298.pdf

Upload the Report Document. File must be a PDF. Please do not password protect or secure the PDF . The maximum file size for the Report Document is 50MB.

SpeyerGTFinalReport.pdf

Upload a Report Document, if any. The maximum file size for the Report Document is 50MB.

Archival Publications (published) during reporting period:

Changes in research objectives (if any):

Change in AFOSR Program Manager, if any:

Extensions granted or milestones slipped, if any:

6 month no-cost extension

AFOSR LRIR Number

LRIR Title

Reporting Period

Laboratory Task Manager

Program Officer

Research Objectives

Technical Summary

Funding Summary by Cost Category (by FY, $K)

	Starting FY	FY+1	FY+2
Salary			
Equipment/Facilities			
Supplies			
Total			

Report Document

Report Document - Text Analysis

Report Document - Text Analysis

Appendix Documents

2. Thank You

E-mail user

Feb 16, 2016 11:14:51 Success: Email Sent to: robert.speyer@mse.gatech.edu